Results for REXI

Martin Schreiber <M.Schreiber@exeter.ac.uk>
et al.

September 4, 2015

This documents is on results for the REXI as described in [2] [3] and is based on the linear formulation only. Several benchmarks are executed to evaluate the dependency of the REXI parameters on scenarios representative for geophysical flows.

1 Benchmark scenario description

1.1 Equations

We analyze the behavior of REXI based on parameter studies of the linear part

$$L(U) := \begin{pmatrix} 0 & -\eta_0 \partial_x & -\eta_0 \partial_y \\ -g\partial_x & 0 & f \\ -g\partial_y & -f & 0 \end{pmatrix} U$$

of the SWE (see [1], note that the sign is inverted)

$$U_t = L(U).$$

If not otherwise stated, we set $g = \eta_0 = f = 1$ and $\Omega = [0;1]^2$.

1.2 Initial conditions

We use the Gaussian function

$$\eta(x,y) = \eta_0 + e^{-50(x^2+y^2)}$$

as initial conditions and use zero values for initial velocity conditions.

1.3 Discretization in time

A Runge-Kutta time stepping method of 4-th order is used if appropriate. E.g. RK4 does not make sense for REXI.

1.4 Discretization in space

The tests are based on different implementations:

1.4.1 Used derivatives

Furthermore, the derivatives can be based on

- (FDderiv) Finite difference methods (e.g. a $[-1,0,1]$ stencil) or
- (SPderiv) computing the derivative via the spectral basis functions ($\frac{d}{dx} e^{ixj2\pi}$).

1.4.2 Realization of operator

Derivatives can be expressed either in

- (Cop) Cartesian space via a stencil computation (expensive in Cartesian space) or
- (Sop) Spectral (Fourier) space via a spectral convolution (element-wise multiplication and hence very cheap in spectral space).

1.4.3 Grid alignment

- (A-grid): All conserved quantities are places at the cell center
- (C-grid): The potential is placed at the cell center and the velocity components at the cell edges

1.4.4 REXI

There is only one REXI implementation, but with different parameters which are discussed below.

1.5 REXI

The REXI approach allows testing different parameters. In this work, we analyze the accuracy of REXI, based on the parameters h and M, see [3] for their description. We denote the result $U'(\tau)$ of the REXI approach by

$$U'(\tau) := REXI(U(0), \tau, h, M)$$

with U the solution at $t = 0$, the parameterτ the size of the large time step, h the sampling interval size and M the number of poles.

1.6 Error norm

We use the RMS error norm

$$rms(f) := \sqrt{\frac{\sum_{\vec{x}} \left(f_{\vec{x}} - \tilde{f}_{\vec{x}}\right)^2}{\prod_i \vec{N}_i}}$$

based on a discrete computed solution $f_{\vec{x}}$ for the points given by $\vec{x}_i \in \{0, 1, ..., \vec{N}_i\}$, the reference solution given by $\tilde{f}(\vec{x})$ and with each component in $\vec{N}$ giving the resolution.

2 Analytical results

2.1 Testing for h/M parameters

(benchmark folder: 2015_08_30_search_h_M)

We first search for an optimal choice of h and M values. h is a value which only relates to the accuracy of the REXI approximation and M relates to the accuracy, as well as to the computational workload which has to be invested for the REXI approach. We execute the simulation for an overall simulation time of one second and use a time step size for REXI of 0.1. Hence, 10 REXI time steps are executed. The results are given based on the computation of the RMS error on the height.

We first analyze a parameter study for a resolution of 128^2.

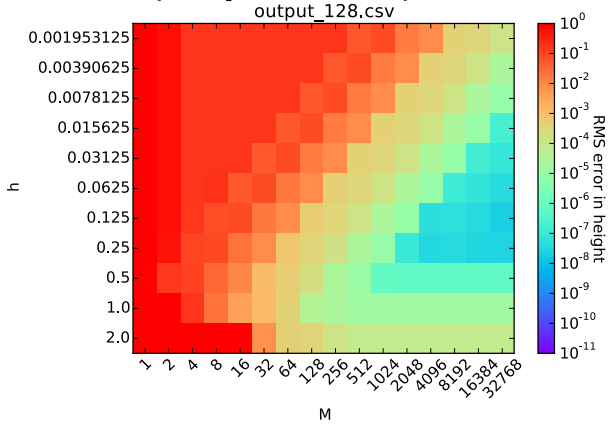

First, we can see a (blue-colored) triangle with high-accurate solutions of $O(10^{-6})$. This optimal triangle area can be described by

$$A_{(M,h)}(C) := \{(M, h) | Mh > C,\ h > 0.5\}$$

with 1024 for an accuracy $\approx 10^{-7}$.

The diagonal edge at $Mh = const.$ is explained by h specifying the sampling interval and M the sampling nodes. If a smaller value of h results in an oversampling of the frequency, more poles M have to be used to accurately cover the approximation of the solution. Since we should try to minimize M as far as possible, we can determine a particular best-investment for M at the left lower corner of the triangle area by choosing $h \in [0.125, 0.25]$.

We define such an optimal choice of h and M as the sweetspot for a given numeric solution $U'(t+\tau) := REXI(U(t), \tau, h, M)$ and a given numerical error threshold$e$. We then search for parameters (M, h) which keep the error below a certain error threshold e and which minimize the number of poles directly related to M.

$$S(h, M) := min_M min_h \left(rms\left(U'(t+\tau) - U(t\tau)\right) < e\right)$$

obviously, the optimal choice of the parameters (M, h).

Next, we test if both parameter change for different resolutions 16^2 and 64^2:

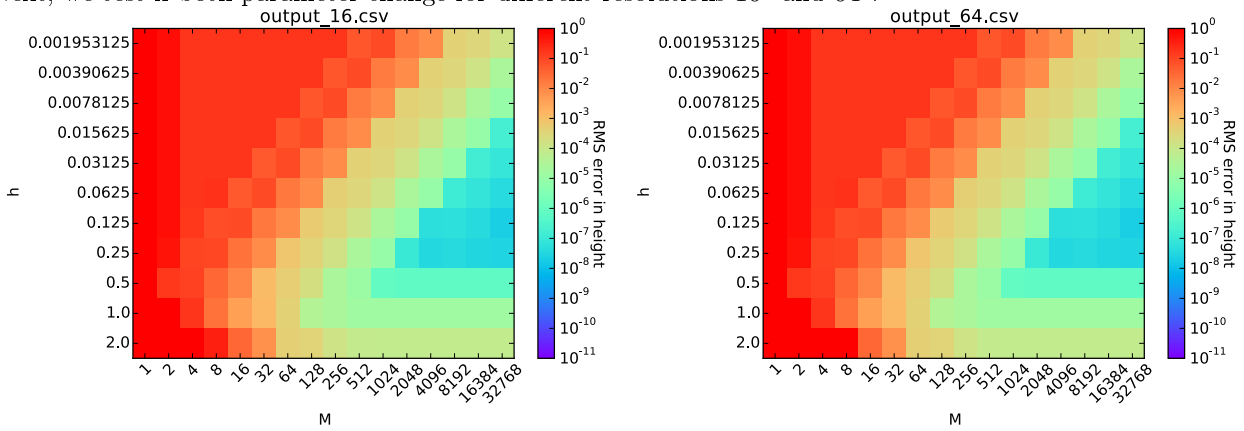

We can observe, that a change in resolution does not significantly change the results for selected parameters h and M.

2.2 Testing for different ϵ

(benchmark folder: 2015_08_30_search_epsilons, 2015_09_03_search_epsilons, 2015_09_03_search_epsilons_b)

The REXI approach should hold for all the possible regimes of atmospheric constellations. Therefore, we generalize our formulation with ϵ

$$U_t = \epsilon L(U)$$

which we realize by setting $g = \eta_0 = f = \epsilon$. We fix our test resolution to 64^2 for this evaluation and show plots for $\epsilon := \{1, 0.1, 0.01\}$:

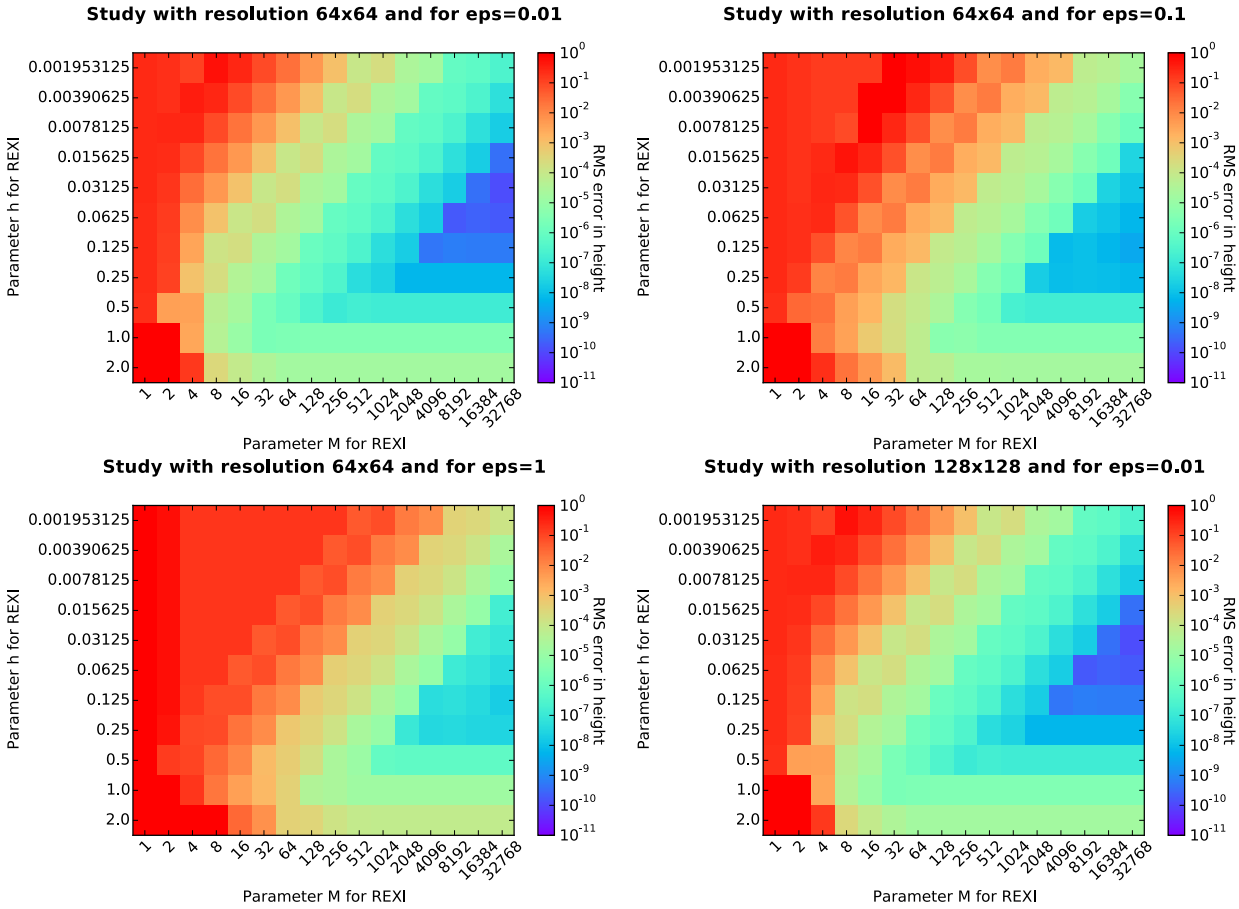

For a decreasing ϵ, we can see that the previously clear optimal parameters for (h, M) are now getting more diffusive. To see if the parameters (h, M) depend on the resolution, we added a plot for benchmarks with the resolution 128^2 and $\epsilon := 0.01$, see above. We can see, that the parameters of the REXI approach are independent to the resolution.

Since the borders got more diffusive for $\epsilon \ll 1$, we expect a sharp border for $\epsilon \gg 1$ which we evaluate next:

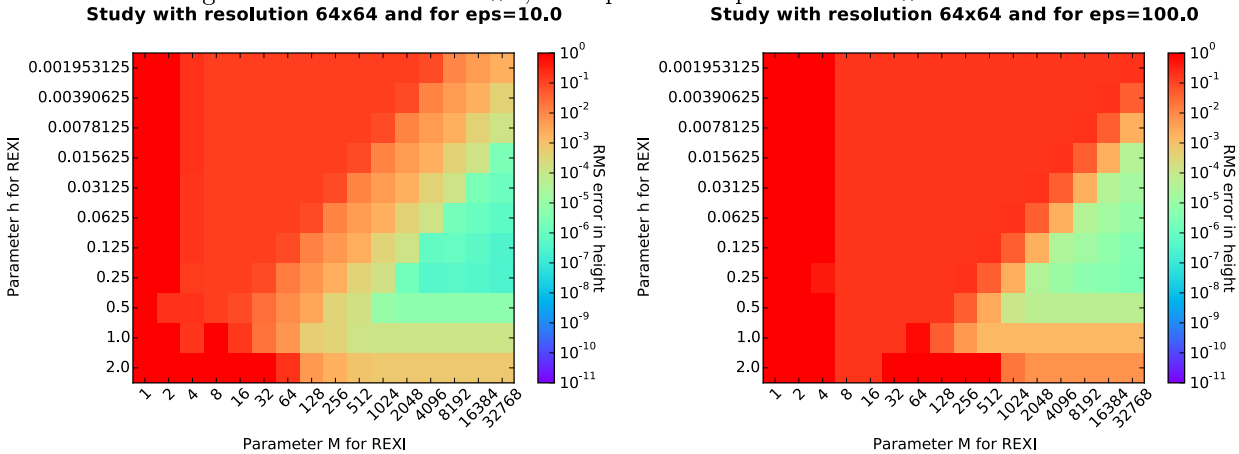

However, we don't see an increase in diffusiveness. But we can observe, that the solution area $A_{(M,h)}$ is shifted to the right side. Hence, for larger ϵ values (this increases the stiffness of the problem), we also have to increase M. We observe again, that the solution area $A_{(M,h)}$ still seems to be independent to the choice of h.

To determine the dependency of M to ϵ, we finally executed a parameter study by setting $h := 0.2$ and with variables ϵ and M. Here, we keep the simulation time limited to 1 second and use a REXI timestep size of $dt := 0.1$.

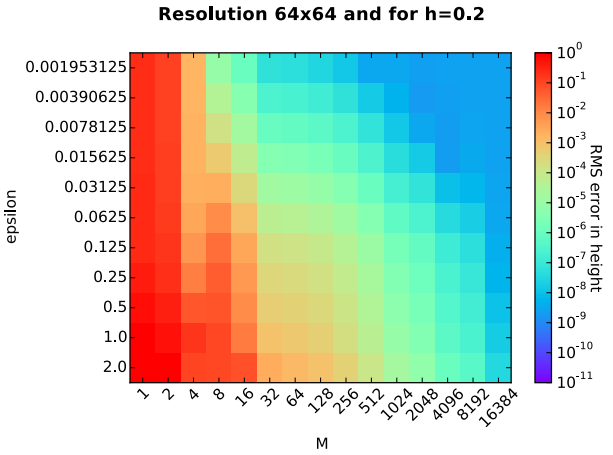

We can see a linear dependency of ϵ to M in the range of$\epsilon \in [0.01; 1]$.

2.3 Increasing large time step

(benchmark folder: 2015_09_02_increasing_large_timesteps)

In theory, we can make very long time steps with the REXI approach. However, the question arises how the (M, h) coefficients are related to the time step size. We evaluate this by setting $h := 0.2$ (see also [2]) and test the accuracy depending on number of poles related to M for different coarse time step sizes. Only a single time step is computed with REXI with the resolutions 64^2 and 128^2.

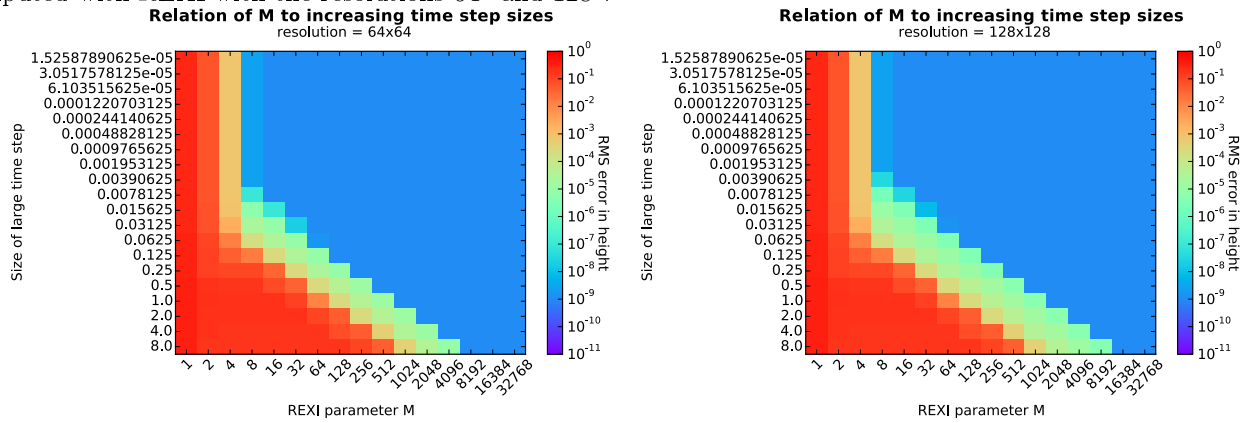

We can observe, that for an increasing large time step size for the REXI approach, also the parameter M increases linearly to the resolution in one dimension:

$$M \sim max_i(\vec{N}_i)$$

with N_i the resolution in dimension i.

Since the parameter M now depends on the resolution, we investigate this in more detail. We set $h : 0.2$ and run parameter studies

2.4 Study for M and N

(benchmark: 2015_09_03_study_N_M)

This study is performed, since M was once stated to depend on N and then that it does not depend on N. Therefore, we investigate this in more detail: We use $h := 0.2$ and vary N and M, showing the heatmap for the RMS accuracy on height in the following plot:

3 Performance benchmarks

Here, we compare the REXI approach with several other possible discretizations, see Sec. 1.4.

3.1 Performance studies for time stepping methods

We executed performance studies on a 40-core Intel Westmere system (4 sockets) to compare the overall computation time of several discretization methods with the REXI approach in both accuracy and time to solution.

[TODO]

3.2 Evaluation via a performance model

With a standard time stepping method, we denote the costs for computing a single time step by $C_N \left(\prod_i \vec{N}_i \right)$. Furthermore, we can assume that $T := O\left(\frac{t \cdot \vec{v}_{max}}{N}\right)$ time steps are required for computing the solution with $\vec{v}_{max} := max_i(\vec{v})$ denoting the maximum velocity.

We assume that M is directly proportional to $\vec{v}_{max}$being related to With the REXI approach, this would result in

For a given M-value, and by using the symmetry of the α_i poles in REXI, this requires solving $L+M+1$ times (TODO: check this) the system $(L-\alpha)^{-1}$.

4 Summary

We summarize

5 Discussion of possible alternative approaches

5.1 Eigenvector decomposition in spectral space

Since the analytical solution is directly given by an Eigenvalue decomposition in spectral space, this could be an appropriate alternative to using the REXI approach. This is true for the f-plane. Let's analyze this property with the β-plane. Here, the f value is not constant over the plane, but varies depending on the y-coordinate:

$$f(y) := f_0 + \beta y$$

We can now have a look at the spectral formulation of the $L(U)$ operator

$$-L(U) := \begin{pmatrix} 0 & \eta_0 \partial_x & \eta_0 \partial_y \\ g\partial_x & 0 & -f(y) \\ g\partial_y & f(y) & 0 \end{pmatrix} U$$

with $U(\vec{x})$ given by its spectral superposition

$$U(\vec{x}) := \int_{\vec{k}} \tilde{U}(\vec{k}) e^{i\vec{k}\vec{x}}$$

and $f(\vec{x})$ given by

$$f(\vec{x}) := \int_{\vec{k}} \tilde{f}(\vec{k}) e^{i\vec{k}\vec{x}}.$$

We were able to compute the solution to $L(U)$ directly in spectral space with the EV decomposition, since we were able to factor out the spectral basis functions. An example is given here for the term $\eta_0 \partial_x$:

$$(\eta_0 \partial_x) \int_{\vec{k}} \tilde{U}(\vec{k}) e^{i\vec{k}\vec{x}} = \int_{\vec{k}} \tilde{U}(\vec{k}) \eta_0 \partial_x e^{i\vec{k}\vec{x}} = \int_{\vec{k}} \tilde{U}(\vec{k}) \eta_0 i\vec{k} e^{i\vec{k}\vec{x}} = \int_{\vec{k}} \tilde{U}(\vec{k}) \left(\eta_0 i\vec{k} e^{i\vec{k}\vec{x}} \right)$$

In combination with a Ritz-Galerkin approach and using the orthogonality of the basis functions, this allows a wave-wise Eigenvalue decomposition. However for the $f(x)$ term, we are not able to factor out the basis function and apply the previously mentioned method

$$(f(y)) \int_{\vec{k}} \tilde{U}(\vec{k}) e^{i\vec{k}\vec{x}} = \int_{\vec{k}} f(\vec{k}) e^{i\vec{k}\vec{x}} \int_{\vec{k}} \tilde{U}(\vec{k}) e^{i\vec{k}\vec{x}}$$

which results in a non-linearity. Hence, we are not able to factor out the spectral basis functions and the approach is not applicable to the β-plane anymore.

References

[1] Formulations of the shallow-water equations, M. Schreiber, P. Peixoto et al.

[2] High-order time-parallel approximation of evolution operators, T. Haut et al.

[3] Understanding the Rational Approximation of the Exponential Integrator (REXI), Schreiber M., Peixoto P.